




# Contrast-enhanced ultrasound features of adrenal lesions in dogs

Silvia Burti<sup>1</sup> | Alessandro Zotti<sup>1</sup> | Giuseppe Rubini<sup>2</sup> | Riccardo Orlandi<sup>3</sup>  |  
 Paolo Bargellini<sup>3</sup> | Federico Bonsembiante<sup>1</sup>  | Barbara Contiero<sup>1</sup> |  
 Margherita Bendazzoli<sup>1</sup> | Tommaso Banzato<sup>1</sup> 

<sup>1</sup>Department of Animal Medicine, Production and Health, University of Padua, Legnaro, Italy

<sup>2</sup>ULTRAVET, San Giovanni in Persiceto, Bologna, Italy

<sup>3</sup>AniCura Tyrus Clinica Veterinaria, Terni, Italy

## Correspondence

Tommaso Banzato, Department of Animal Medicine, Production and Health, University of Padua, Viale Dell'Università 16, Legnaro, Italy.  
 Email: [tommaso.banzato@unipd.it](mailto:tommaso.banzato@unipd.it)

## Funding information

Department of Animal Medicine, Production and Health—MAPS, University of Padua, Italy, Grant/Award Numbers: SID Banzato 2019, DOR Banzato 2022

## Abstract

**Background:** The contrast-enhanced ultrasound (CEUS) features of adrenal lesions are poorly reported in veterinary literature.

**Methods:** Qualitative and quantitative B-mode ultrasound and CEUS features of 186 benign (adenoma) and malignant (adenocarcinoma and pheochromocytoma) adrenal lesions were evaluated.

**Results:** Adenocarcinomas ( $n = 72$ ) and pheochromocytomas ( $n = 32$ ) had mixed echogenicity with B-mode, and a non-homogeneous aspect with a diffused or peripheral enhancement pattern, hypoperfused areas, intralesional microcirculation and non-homogeneous wash-out with CEUS. Adenomas ( $n = 82$ ) had mixed echogenicity, isoechogenicity or hypoechogenicity with B-mode, and a homogeneous or non-homogeneous aspect with a diffused enhancement pattern, hypoperfused areas, intralesional microcirculation and homogeneous wash-out with CEUS. With CEUS, a non-homogeneous aspect and the presence of hypoperfused areas and intralesional microcirculation can be used to distinguish between malignant (adenocarcinoma and pheochromocytoma) and benign (adenoma) adrenal lesions.

**Limitations:** Lesions were characterised only by means of cytology.

**Conclusions:** CEUS examination is a valuable tool for distinction between benign and malignant adrenal lesions and can potentially differentiate pheochromocytomas from adenocarcinomas and adenomas. However, cytology and histology are necessary to obtain the final diagnosis.

## KEYWORDS

adenoma, adrenal lesion, contrast-enhanced ultrasound, cytology, dog

## INTRODUCTION

Adrenal tumours (ATs) are reported to be uncommon in dogs, accounting for just 0.17%–0.76% of all neoplasms in this species. ATs can be benign or malignant and can result in a vast array of clinical signs due to hormone secretion or invasion of adjacent organs (mainly the caudal vena cava). AT can be suspected based on clinical findings when, for example, Cushing-like syndromes or systemic hypertension are evident.<sup>1</sup> On the other hand, AT is often an incidental finding during ultrasonographic (US) or computed tomographic (CT) scans performed to investigate unrelated

pathologies.<sup>1–3</sup> In such a scenario, it is easily understood that the diagnosis and management of ATs is not straightforward and often requires a multimodal approach. Identification of the lesion histotype is paramount to determining the correct therapy, if any.

Adrenal glands are mainly investigated by means of US<sup>4</sup> and CT,<sup>5</sup> but some recent reports on the magnetic resonance imaging features of normal adrenal glands in dogs are also available.<sup>6</sup> To date, several reports assessing the normal dimensions of adrenal glands in dogs, as measured by US, have been published,<sup>7</sup> and a cut-off value of 20 mm for differentiating benign

This is an open access article under the terms of the [Creative Commons Attribution-NonCommercial](https://creativecommons.org/licenses/by-nc/4.0/) License, which permits use, distribution and reproduction in any medium, provided the original work is properly cited and is not used for commercial purposes.

© 2023 The Authors. *Veterinary Record* published by John Wiley & Sons Ltd on behalf of British Veterinary Association.

from malignant lesions has been reported by several authors.<sup>1,8</sup> Furthermore, other B-mode features, such as vascular invasion and irregular shape, are also reported to be associated with malignancy.<sup>8</sup>

Contrast-enhanced ultrasound (CEUS) has gained some popularity in the last few years. The normal and pathological aspects of several abdominal organs in dogs, such as the liver, spleen, intestine and pancreas, have been published,<sup>9–13</sup> while the CEUS features of normal adrenal glands have been described in six dogs.<sup>14</sup> In five of the six dogs, a peculiar second homogeneous enhancement peak, evident 30–40 seconds after the injection of contrast medium, was described by the authors. Furthermore, both B-mode ultrasound and CEUS have shown some promising results in the differentiation between different AT types.<sup>2,15,16</sup> Nevertheless, these studies were based on a relatively small number of cases; in particular, Bargellini et al.<sup>15</sup> included 16 cases, whereas Pey et al.<sup>16</sup> included 24 cases. A more recent paper describing the CEUS features of 45 ATs in dogs reports a limited utility of this technique in the differentiation between cortical adenoma (CA), cortical adenocarcinoma (CAC) and pheochromocytoma (PHEO). This latter study was performed using Sonazoid (Daiichi—Sankyo Corp., Tokyo, Japan), a contrast agent that is not commercially available on the European or the American market; therefore, the results are not immediately applicable in such scenarios.<sup>2</sup>

Based on the above assertions, the aims of this study were (1) to describe the B-mode and CEUS features of ATs in dogs based on a large (186) dataset of lesions; (2) to develop an easy-to-use machine learning-based decision tree to help the clinician in the prediction of the AT histotype; and (3) to compare the results of this study with those reported in the literature.

## METHODS

### Cases

A total of 182 dogs referred, between January 2008 and June 2021, to AniCura Tyrus Veterinary Clinic (Terni, Italy), Ultravet (San Giovanni in Persiceto, Bologna, Italy) and the Veterinary Teaching Hospital at the University of Padua (O.V.U.D., Padova, Italy) with previously identified adrenal gland lesions were retrospectively selected by G. R. and S. B. CEUS and cytopathological examination of the adrenal lesions were performed in all the patients. Only cases with a definitive cytopathological diagnosis were included. Complete signalment and medical history were recorded for each dog.

All the methods were applied in accordance with the relevant guidelines and regulations. This study was conducted respecting Italian Law No. 26/2014 (that transposes the EU directive 2010/63/EU). As the data used in this study were collected during routine clinical activity, no ethical committee approval was needed. Informed consent for personal data processing was obtained from the owners.

## B-mode ultrasound and CEUS

A complete B-mode US examination of the abdomen and a CEUS examination of the adrenal glands were performed on each animal by two veterinarians (G. R. and P. B., with 19 and 16 years of experience in small animal US, respectively). Four different ultrasound scanners (GE Logic E9 [GE Medical Systems], Esaote MyLab70 Gold [Esaote Italia], Esaote Twice [Esaote Italia] and Philips Affiniti 50 [Italy]) were used.

An 8-hour fasting period prior to examination was respected for each dog, and sedation with butorphanol tartrate<sup>17</sup> was administered intramuscularly in restless cases. SonoVue (Bracco Imaging, Geneva, Switzerland) was administered intravenously at a dose of 0.05 mL/kg, followed by a 5 mL saline flush through a three-way stopcock with an extension tube (containing 0.5 mL of fluid) directly connected to the intravenous cannula. Each lesion was scanned continuously for at least 1 minute or until the end of the wash-out phase. The mechanical index was set to a low value (0.02). Each scan was fully recorded.

## Qualitative and quantitative analysis

All the B-mode and CEUS examinations were reviewed by the same two veterinarians (G. R. and S. B.). The following qualitative B-mode features of the lesions were evaluated: (1) echogenicity (anechoic, hypoechoic, isoechoic, hyperechoic or mixed echogenicity) and (2) acoustic enhancement (present or absent). This latter feature was included because acoustic enhancement can be related to the presence of cystic areas, possibly having necrotic or haemorrhagic content. If the lesion involved only one of the two poles, the echogenicity was compared with that of the remainder of the adrenal gland. If the lesion involved the entire gland, the echogenicity was compared with that of the adjacent fat. The echogenicity of the lesion was defined as mixed when both hypoechoic and hyperechoic areas were detected. The maximum diameter of the focal lesions was evaluated during B-mode examination.

The following qualitative CEUS features were evaluated during the wash-in phase<sup>12,15</sup>: (1) homogeneity of the lesion (homogeneous or non-homogeneous); (2) distribution of the contrast medium (diffused, peripheral or central); (3) hypoperfused areas (present or absent); (4) intralesional microcirculation (present or absent); (5) vascularisation pattern of microcirculation (centripetal, centrifugal, disordered or nodular). During the wash-in phase, vascular invasion was also evaluated.

The following qualitative features were evaluated during the wash-out phase<sup>12,15</sup>: (1) wash-out (present or absent); (2) redistribution of the contrast medium (present or absent); (3) homogeneity of the lesion (homogeneous or non-homogeneous). Redistribution of the contrast medium was classified as present when the hypoperfused areas disappeared or decreased in size and/or number after the wash-in peak.

The following quantitative CEUS features of the lesions were evaluated<sup>12,15</sup>: (1) time to enhancement (TTE), which was the timespan between injection and appearance of the signal in the lesion; (2) time to peak (TTP), which was the timespan between injection and the peak intensity of the signal; (3) time to wash-in (TTWI), calculated as TTP minus TTE. When redistribution was evident, the time to redistribution was also calculated as the timespan occurring between injection and the maximum distribution of the contrast medium.

The qualitative features of the individual lesions were classified after consensus discussion. More specifically, after individual completion of the description, consensus between the two evaluators was used to assign the final features.

To reduce digital storage consumption, all the CEUS examinations were stored as audio video interleave (AVI) files, and the original digital imaging and communication in medicine files were no longer available. The time–intensity curves used to extract the quantitative CEUS features from the AVI files were calculated using a custom-built MATLAB script developed by one of the authors (T. B.).

## Adrenal gland lesion classification

Adrenal gland lesions were sampled by means of US-guided fine-needle aspiration. Cytological slides were air-dried and stained with May–Grünwald–Giemsa stain. All the cytological slides were evaluated by a trained clinical pathologist (F. B.) and classified as CAC, CA or PHEO based on previously published cytopathological criteria.<sup>18,19</sup> In addition, a diagnosis of adrenocortical tumour was made when the neoplastic cells were present in cohesive clusters with distinct cell borders and had basophilic, markedly vacuolated cytoplasm and a round-to-oval and central-to-peripheral nucleus, with coarse or condensed chromatin. Among the adrenocortical tumours, a lesion was diagnosed as CAC when neoplastic cells showed features that were highly suggestive of cellular atypia, such as moderate-to-marked anisocytosis and anisokaryosis, multiple nucleoli and atypical mitoses. In the case of caudal vena cava or renal artery invasion, the lesion was classified as CAC even if no features suggestive of cellular atypia were evident on cytopathology. CA was diagnosed when no features suggestive of cellular atypia were evident on cytopathology and if no vascular invasion was detected. The lesion was classified as PHEO when the cytological slides were composed of naked, round-to-oval nuclei on a background of finely granular and pale basophilic cytoplasm.

## Statistics and data analysis

To compare the differences between the three diagnostic categories, the count data expressed as percentages were analysed with a chi-square test (or Fisher's exact test when there were fewer than five

units of data). The quantitative variables were assessed for normality using the Shapiro–Wilk test. Differences among the three diagnostic categories were analysed with one-way ANOVA for normally distributed data, whereas the non-parametric Kruskal–Wallis test was used for non-normally distributed data. Post hoc pairwise comparisons were calculated with Bonferroni correction. A *p*-value less than 0.05 was considered as statistically significant. The analysis was conducted with SAS 9.4 (SAS Institute Inc., Cary, NC, USA). The 95% confidence intervals (95% CIs) were estimated with Sergeant (Epitools Epidemiological Calculators, ESG, 2018 Ausvet, <https://epitools.ausvet.com.au/ciproportion>).

Thereafter, the dataset was randomly split into a training set comprising two-thirds of the cases ( $n = 124$ ) and a test set comprising the remaining records ( $n = 62$ ). A decision-tree analysis was then performed on the training set to detect the CT features capable of identifying the three diagnostic categories. A recursive partitioning method was adopted using the 'rpart' package of R (<https://cran.r-project.org/web/packages/rpart/vignettes/longintro.pdf>), and a three-step procedure was applied to build the decision tree: (1) the features that provided the best data splitting were selected; (2) a 10-fold cross-validation was used to prune the decision tree in order to obtain the lowest number of branches and the lowest misclassification rate; (3) the decision tree was used to classify the cases in the test set and, thereafter, a confusion matrix ('caret' confusion Matrix function of R library) was built on the test set by comparing the actual versus the predicted histopathological category, and some quality indices (such as sensitivity, specificity and accuracy by category) regarding model performance were calculated. These last analyses were performed with R-software (version 3.6.1).

## RESULTS

### Cytopathological examination

A total of 186 adrenal lesions were present in the 182 dogs referred. The lesions were classified into three categories based on cytopathological diagnosis: 72 CACs, 32 PHEOs and 82 CAs. The right adrenal gland in 70 cases was involved, and in 116 cases, the lesion was localised on the left adrenal gland. In four patients, both adrenal glands were involved (one case of CA in the right adrenal gland and PHEO in the left adrenal gland; two cases of bilateral CA; one case of CAC in the right adrenal gland and CA in the left adrenal gland).

### B-mode ultrasound and CEUS

The B-mode and CEUS features of each cytopathological category are described below. The qualitative and quantitative B-mode and CEUS features are reported in Tables 1–3 and 4, respectively. Caudal vena cava invasion was evident in 23 cases. In addition,

**TABLE 1** Qualitative B-mode features of the lesions, along with cytopathological classification

B-mode features	Adenocarcinoma (n = 72)	Pheochromocytoma (n = 32)	Adenoma (n = 82)	Total (n = 186)	p-Value
<b>Echogenicity*</b>					<0.001
Hypoechoic <sup>+</sup> (n = 19)	3% (1%–10%) <sup>b</sup>	9% (3%–24%) <sup>ab</sup>	17% (10%–27%) <sup>a</sup>	10% (7%–15%)	0.014
Mixed <sup>+</sup> (n = 128)	87% (78%–93%) <sup>a</sup>	75% (58%–87%) <sup>a</sup>	50% (39%–60%) <sup>b</sup>	69% (62%–75%)	<0.001
Hyperechoic (n = 17)	6% (2%–13%)	9% (3%–24%)	12% (7%–21%)	9% (6%–14%)	0.361
Isoechoic (n = 22)	4% (1%–11%) <sup>b</sup>	7% (2%–20%) <sup>ab</sup>	21% (13%–31%) <sup>a</sup>	12% (8%–17%)	0.004
Anechoic (n = 0)	–	–	–		
<b>Presence of acoustic enhancement<sup>+</sup> (n = 49)</b>	39% (28%–50%) <sup>a</sup>	41% (25%–58%) <sup>a</sup>	10% (5%–18%) <sup>b</sup>	26% (20%–33%)	<0.001

Note: Different letters along rows mean significant different value for  $p < 0.05$ .

n is the number of cases.

\*Fisher's exact test.

<sup>+</sup>k-Proportion test.

**TABLE 2** Qualitative contrast-enhanced ultrasound (CEUS) wash-in features, along with cytopathological classification of the lesions

CEUS wash-in	Adenocarcinoma (n = 72)	Pheochromocytoma (n = 32)	Adenoma (n = 82)	Total (n = 186)	p-Value
<b>Homogeneity<sup>+</sup> (n = 58)</b>	11% (6%–20%) <sup>b</sup>	12% (5%–28%) <sup>b</sup>	56% (45%–66%) <sup>a</sup>	31% (25%–38%)	<0.001
<b>Distribution*</b>					0.368
Diffuse <sup>+</sup> (n = 138)	71% (59%–80%)	66% (48%–80%)	80% (71%–88%)	74% (67%–80%)	0.187
Peripheral <sup>+</sup> (n = 40)	24% (15%–35%)	31% (18%–49%)	16% (9%–25%)	22% (16%–28%)	0.170
Central <sup>+</sup> (n = 8)	5% (2%–13%)	3% (1%–16%)	4% (1%–10%)	4% (2%–8%)	0.793
<b>Presence of hypoperfused areas<sup>+</sup> (n = 134)</b>	94% (87%–98%) <sup>a</sup>	75% (58%–87%) <sup>a</sup>	51% (41%–62%) <sup>b</sup>	72% (65%–78%)	<0.001
<b>Presence of intralesional microcirculation<sup>+</sup> (n = 106)</b>	81% (70%–88%) <sup>a</sup>	56% (39%–72%) <sup>ab</sup>	37% (27%–47%) <sup>b</sup>	57% (50%–64%)	<0.001
<b>Vascularisation pattern*</b>					0.221
Centrifugal <sup>+</sup> (n = 4)	5% (2%–14%)	–	3% (0.6%–17%)	4% (1%–9%)	0.596
Centripetal <sup>+</sup> (n = 11)	10% (5%–21%)	17% (6%–39%)	7% (2%–21%)	10% (6%–18%)	0.546
Disordered <sup>+</sup> (n = 88)	84% (73%–92%)	83% (61%–94%)	80% (63%–90%)	83% (75%–89%)	0.868
Nodular <sup>+</sup> (n = 3)	–	–	10% (3%–26%)	3% (1%–8%)	0.200

Note: Different letters along rows mean significant different value for  $p < 0.05$ .

n is the number of cases.

\*Fisher's exact test.

<sup>+</sup>k-Proportion test.

**TABLE 3** Qualitative contrast-enhanced ultrasound (CEUS) wash-out features, along with cytopathological classification of the lesions

CEUS wash-out	Adenocarcinoma (n = 72)	Pheochromocytoma (n = 32)	Adenoma (n = 82)	Total (n = 186)	p-Value
<b>Presence of wash-out<sup>+</sup> (n = 125)</b>	57% (45%–68%) <sup>b</sup>	91% (76%–97%) <sup>a</sup>	67% (56%–76%) <sup>b</sup>	67% (60%–73%)	0.003
<b>Presence of redistribution<sup>+</sup> (n = 45)</b>	33% (23%–45%)	16% (7%–32%)	20% (12%–29%)	24% (19%–31%)	0.063
<b>Homogeneity<sup>+</sup> (n = 68)</b>	19% (12%–30%) <sup>b</sup>	12% (5%–28%) <sup>b</sup>	61% (50%–71%) <sup>a</sup>	37% (30%–44%)	<0.001

Note: Different letters along rows mean significant different value for  $p < 0.05$ .

n is the number of cases.

<sup>+</sup>k-Proportion test.

invasion of the phrenic-abdominal vena was seen in five cases, and invasion of the renal vein was detected in one case.

## Adenocarcinoma

CACs mainly showed mixed echogenicity (87%) on B-mode ultrasound, and acoustic enhancement was

evident in only 39% of cases. On CEUS examination, CACs were mainly non-homogeneous (89%) nodules characterised by either diffused (71%) or peripheral (24%) distribution of the contrast medium. Hypoperfused areas and intralesional microcirculation (94% and 81%, respectively) were almost always evident during the wash-in phase. Intralesional microcirculation showed mainly (85%) a disordered vascularisation pattern. Wash-out was evident in 57% of cases.



**TABLE 4** Quantitative contrast-enhanced ultrasound wash-in features, along with cytopathological classification of the lesions

	<b>Adenocarcinoma (n = 72)</b>	<b>Pheochromocytoma (n = 32)</b>	<b>Adenoma (n = 82)</b>	<b>Total (n = 186)</b>	<b>p-Value</b>
<b>Maximum dimension<sup>+</sup> (cm)</b>	3.0 (2.0–4.0) <sup>a</sup>	2.7 (2.1–3.8) <sup>a</sup>	1.4 (1.0–2.0) <sup>b</sup>	2.1 (1.4–3.3)	<0.001
<b>TTE<sup>+</sup> (seconds)</b>	8.0 (6.0–11.5) <sup>a</sup>	7.0 (6.0–10.0) <sup>ab</sup>	7.0 (6.0–9.0) <sup>b</sup>	7.0 (6.0–10.0)	0.039
<b>TTP<sup>+</sup> (seconds)</b>	16.0 (12.0–21.0) <sup>a</sup>	12.0 (10.0–16.0) <sup>b</sup>	13.0 (11.0–18.0) <sup>ab</sup>	14.0 (11.0–18.0)	0.009
<b>TTWI<sup>+</sup> (seconds)</b>	7.0 (5.0–9.5) <sup>a</sup>	5.0 (4.0–6.0) <sup>b</sup>	6.0 (5.0–8.0) <sup>a</sup>	6.0 (4.0–8.0)	0.002
<b>Redistribution time* (seconds)</b>	25.9 (±8.0)	25.6 (±5.7)	30.7 (±7.9)	27.6 (±8.0)	0.148

Note: n is the number of cases.

Abbreviations: TTE, time to enhancement; TTP, time to peak; TTWI, time to wash-in.

<sup>a</sup>Kruskal–Wallis test; data are presented as median (interquartile range).

\*One-way ANOVA; data are reported as mean (±standard deviation).

During the wash-out phase, CACs were mostly non-homogeneous (81%) lesions showing redistribution of contrast medium in only 33% of cases. Vascular invasion was evident in 13 cases, always involving the caudal vena cava. Involvement of the phrenic-abdominal vein and of the renal vein was evident in two cases and one case, respectively.

## Pheochromocytoma

PHEOs were mostly characterised by a mixed echogenicity (75%) on B-mode examination, and acoustic enhancement was evident in 41% of cases. During the wash-in phase, CACs were non-homogeneous (88%) nodules showing either diffused (66%) or peripheral (31%) contrast medium distribution patterns. Hypoperfused areas were present in 75% of cases. Intralesional microcirculation characterised mainly by a disordered pattern was seen in 56% of cases. The wash-out phase was almost always evident (91%), with the lesions being more frequently non-homogeneous (88%). The caudal vena cava was clearly invaded in 10 cases, and the phrenic-abdominal vein was also involved in three cases.

## Adenoma

Adrenal CAs showed mostly mixed echogenicity (50%), isoechogenicity (21%) and hypoechogenicity (17%) on B-mode examination. During the wash-in phase of the CEUS examination, CAs were both homogeneous (56%) and non-homogeneous (44%) lesions characterised by diffused (80%) distribution of the contrast medium. Hypoperfused areas were evident in 51% of cases. Intralesional microcirculation, showing mainly a disordered pattern (80% of cases), was seen in 37% of cases. During the wash-out phase (evident in 67% of cases), CAs appeared as homogeneous (61%) lesions with redistribution of the contrast medium present in 20% of cases. Vascular invasion was never evident.

## Statistical analysis

Among the B-mode features, both echogenicity ( $p < 0.001$ ) and the presence of acoustic enhancement ( $p < 0.001$ ) showed statistically significant differences. In particular, mixed echogenicity was the most

common presentation among all the adrenal lesions (69%,  $p < 0.001$ ), whereas acoustic enhancement was evident only in 26% of the lesions, with CAC (39%) and PHEO (41%) being the most represented cytopathological categories. No difference in the distribution of hyperechoic lesions among the different cytopathological groups was evident ( $p = 0.361$ ).

Among the wash-in features, statistically significant differences were evident for homogeneity ( $p < 0.001$ ), presence of hypoperfused areas ( $p < 0.001$ ) and presence of intralesional microcirculation ( $p < 0.001$ ). Among the wash-out features, presence of wash-out ( $p = 0.003$ ) and homogeneity ( $p < 0.001$ ) showed statistically significant differences among the different cytopathological groups, whereas no differences were evident for the remaining features.

Among the quantitative features, the maximum dimension ( $p < 0.001$ ), TTE ( $p = 0.039$ ), TTP ( $p = 0.009$ ) and TTWI ( $p = 0.002$ ) showed statistically significant differences. No significant differences were evident for redistribution time ( $p = 0.148$ ). Representative B-mode and CEUS images of each of the included cytopathological categories of adrenal lesions are shown in Figures 1–3.

The decision tree for classifying adrenal lesions included presence of intralesional microcirculation, echogenicity and homogeneity during wash-in among the qualitative features and only TTWI among the quantitative features. A total of 19 of the 25 CACs were correctly classified, while five of the remaining CACs were classified as CAs and one as PHEO. Only three of the 14 PHEOs were correctly classified. The remaining PHEOs were classified as seven cases of CAC and four cases of CA. Lastly, 17 of the 23 CA cases were correctly classified, and the remaining six were misclassified as CAC.

The overall accuracy of the test-set decision tree was 0.63 (95% CI 0.50–0.75). The confusion matrix, sensitivity, specificity and balanced accuracy for each cytopathological category as classified by both decision-tree sets are reported in Table 5. The developed decision tree is depicted in Figure 4.

## DISCUSSION

The results of the present study suggest that there are no specific CEUS features that can be clearly

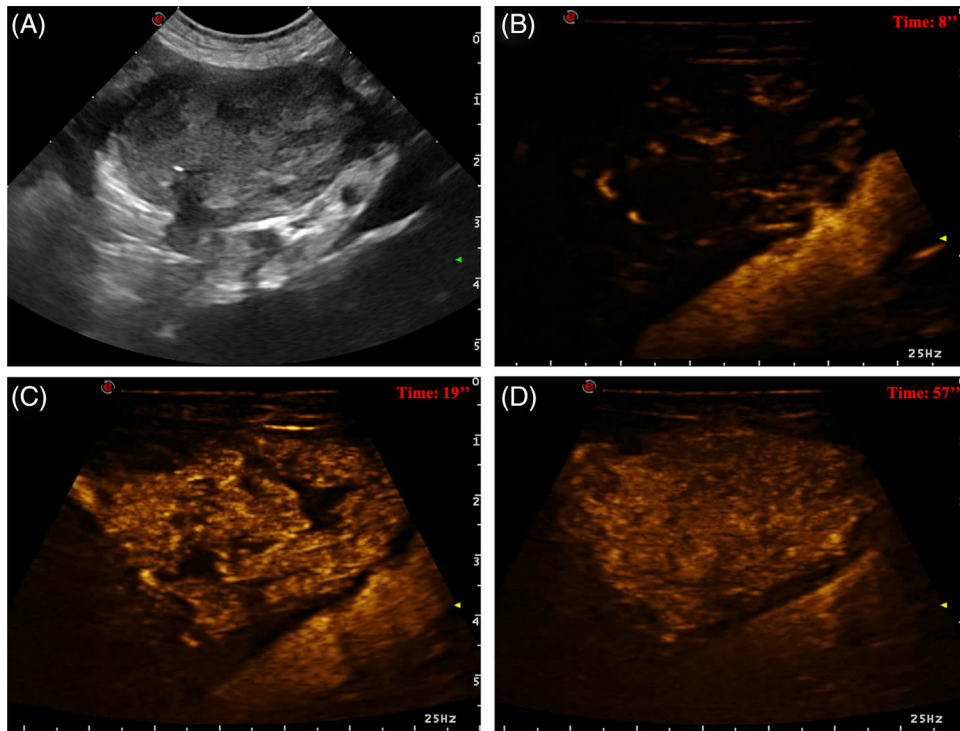


**FIGURE 1** Example of an adenocarcinoma showing mixed echogenicity with presence of acoustic enhancement at ultrasonography (US), and diffused and non-homogeneous distribution of the contrast medium, with presence of hypoperfused areas and disordered intralesional microcirculation during the wash-in phase at contrast-enhanced ultrasound. Wash-out is present, with a non-homogeneous aspect. (A) Image obtained from US examination; (B) image obtained at time to enhancement; (C) image obtained at time to peak; (D) image obtained during the wash-out phase

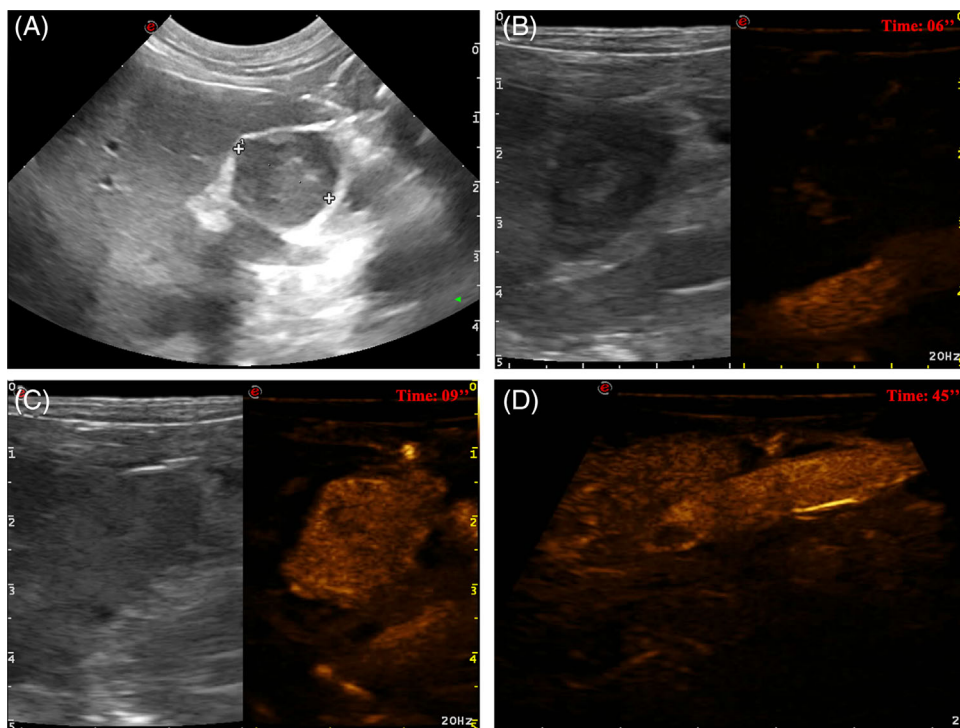


**FIGURE 2** Example of a pheochromocytoma showing mixed echogenicity with presence of acoustic enhancement at ultrasonography (US), and diffused and non-homogeneous distribution of the contrast medium, with presence of hypoperfused areas during the wash-in phase at contrast-enhanced ultrasound. Wash-out is present, with a non-homogeneous aspect. (A) Image obtained from US examination; (B) image obtained at time to enhancement; (C) image obtained at time to peak; (D) image obtained during the wash-out phase

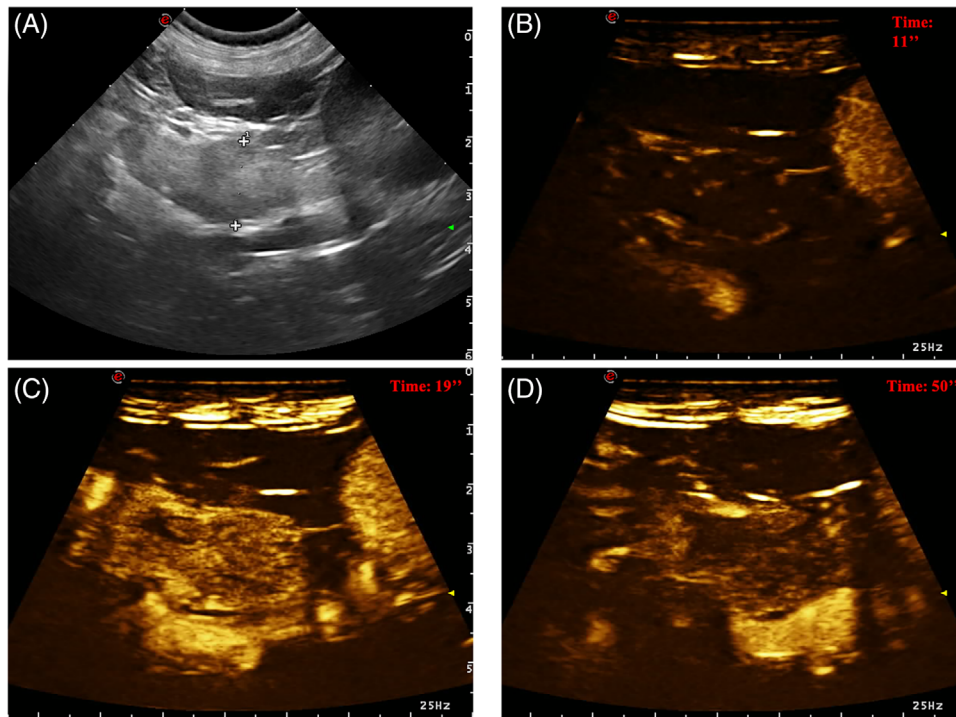


**FIGURE 3** Example of an adenoma showing mixed echogenicity with absence of acoustic enhancement at ultrasonography (US), and diffused and non-homogeneous distribution of the contrast medium, with presence of hypoperfused areas and disordered intralesional microcirculation during the wash-in phase at contrast-enhanced ultrasound. Wash-out is absent, with a non-homogeneous aspect during wash-out. (A) Image obtained from US examination; (B) image obtained at time to enhancement; (C) image obtained at time to peak; (D) image obtained during the wash-out phase

associated with any of the included cytopathological categories. For instance, malignant lesions, namely, CACs and PHEOs, mainly showed a non-homogeneous aspect on CEUS, and CAs showed both homogeneous and non-homogeneous aspects. A homogeneous aspect on CEUS examination is reported to be highly associated with benign adrenal lesions.<sup>16</sup> In the same way, most of the CACs and PHEOs showed both hypoperfused areas and intralesional microcirculation, likely resulting from the presence of haemorrhagic/necrotic areas and tumour neoangiogenesis. On the other hand, hypoperfused areas and intralesional microcirculation were also present in 51% and 37% of CA cases, respectively. Interestingly, the different distribution of intralesional microcirculation was used for the distinction between CAC and CA on the first branch of the developed decision tree.

In a study by Nagumo et al.<sup>2</sup> including 44 dogs diagnosed with CA (six), CAC (12) and PHEO (26), the authors reported PHEO as having a significantly lower mean transit time compared to both CAC and CA. In other words, in their study, PHEO had a fast wash-in followed by a seemingly fast wash-out. Likewise, PHEO is also reported in Bargellini et al.<sup>15</sup> to have a shorter contrast-enhancement transit time compared to both CA and CAC. The results reported in our study confirm this finding. Indeed, PHEO showed a quick distribution of contrast medium followed by a quick and evident wash-out in 91% of the cases. Furthermore, the TTWI value calculated on PHEOs was significantly lower than the TTWI of the remaining cytopathological categories. It is the authors' opinion that such a

quick transit of the contrast medium could suggest the presence of a more conspicuous microcirculation—both arterial and venous—in PHEOs than in CAs and CACs. This is of course just a hypothesis and would need appropriate studies to be confirmed. Due to the large overlap in the confidence intervals among the different cytopathological categories, such a theoretical explanation requires caution. Nevertheless, it deserves specific histopathological studies.

The presence of hypoperfused areas is reported as a common CEUS feature of CACs both by Bargellini et al.<sup>15</sup> and Pey et al.<sup>16</sup> Furthermore, Pey et al.<sup>16</sup> also reported the presence of tortuous centripetal vessels in some cases (4/10) of CAC. Such findings have been only partially confirmed by our study. Indeed, hypoperfused areas and intralesional microcirculation were present in 94% and 81% of CACs, respectively, but these features were also frequently evident in PHEOs and CAs. As a consequence, the presence of hypoperfused areas and intralesional microcirculation do not enable the differentiation of CAC from the other included cytopathological categories. Nevertheless, evaluating perfusion patterns is a subjective process that depends on the operator's expertise.

CAs are reported in the literature<sup>15,16</sup> as hypoechoic lesions during B-mode examination and as homogeneous and hypoenhancing lesions during CEUS examination. In our study, CAs more frequently showed mixed echogenicity, as did the included malignant lesions (CACs and PHEOs). The presence of acoustic enhancement was recorded only in 15% of CA cases.

In a previous study by Ohlerth and O'Brien,<sup>20</sup> CEUS was reported to be more sensitive compared to colour



**TABLE 5** Confusion matrix, sensitivity, specificity and balanced accuracy of test-set decision tree

Prediction	Reference		
	Adenocarcinoma ( <i>n</i> = 25)	Pheochromocytoma ( <i>n</i> = 14)	Adenoma ( <i>n</i> = 23)
Adenocarcinoma ( <i>n</i> = 25)	19	7	6
Pheochromocytoma ( <i>n</i> = 14)	1	3	0
Adenoma ( <i>n</i> = 23)	5	4	17
Sensitivity	0.76	0.21	0.74
Specificity	0.65	0.99	0.77
Balanced accuracy	0.70	0.60	0.75

Note: *n* is the number of cases.

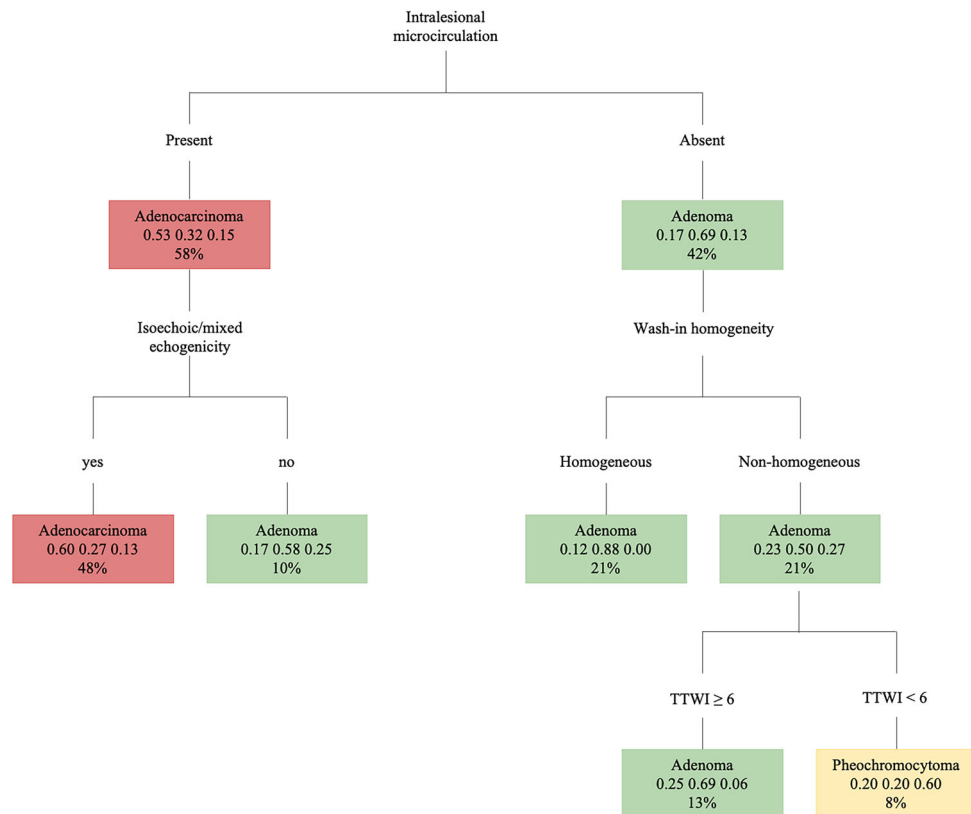


**FIGURE 4** The machine learning-based decision tree developed using the qualitative and the quantitative contrast-enhanced ultrasound features of the adrenal lesions. The probability of each class at a specific node is reported in the second line in each box. The percentage of observations used at that node is reported in the third line in each box. TTWI, time to wash-in

and power Doppler US when examining vascular patterns in small parenchymal vessels. The normal contrast-enhancement pattern of adrenal glands is often (not always) reported as biphasic, with a second peak of contrast medium enhancement between 30 and 40 seconds after injection of the contrast medium.<sup>14</sup> The results of the present study only partially confirm what is reported in the literature. Indeed, a redistribution of the contrast medium, even without a second increase in the signal, was evident only in 45 cases (24 CACs, 16 CAs, five PHEOs), with no significant difference between cytopathological categories for both presence and redistribution time. On the other hand, redistribution of the contrast medium was visible during the late arterial/early venous phase in each case. A feasible explanation for such an unusual feature of adrenal lesions is related to a pos-

sible redistribution of the contrast medium between arterial and venous microcirculation of the adrenal glands.

Following the proposed machine learning-based decision tree, the first CEUS feature used for differentiation among the different cytopathological categories is intralesional microcirculation, particularly for the distinction between CAC (presence of microcirculation) and CA (absence of microcirculation). Nonetheless, only 58% of CACs were classified as such following the first branch of the decision tree. The last branch of the decision tree identified a TTWI value of 6 seconds as cut-off for distinguishing between CA and PHEO, with PHEOs showing a TTWI of less than 6 seconds. Interestingly, a similar cut-off value (mean transit time of 6.2 milliseconds) was reported in the study by Nagumo et al.<sup>2</sup> for the distinction between



PHEO and CAC. Hence, the proposed decision tree has an overall low accuracy (0.53, 95% CI 0.50–0.75).

In human medicine, Hounsfield unit (HU) values less than 10 are reported as a useful cut-off for distinguishing CAs from other ATs. This is related to the relatively higher intracytoplasmic lipid content of CAs. The same result has not been confirmed in the veterinary field.<sup>21</sup> The CT features of canine adrenal lesions reported in the veterinary literature are inconsistent.<sup>21,22</sup> Indeed, Gregori et al.<sup>22</sup> described a large overlapping of CT features among different tumour types. On the contrary, Yoshida et al.<sup>21</sup> reported that PHEO may be distinguished from CA and CAC based on HU values during precontrast scans and venous and delayed phases. To date, based on the results reported on CT and CEUS, none of these diagnostic techniques alone may enable a highly accurate distinction between the different adrenal lesions.

One limitation of this study is that comparison between the findings presented here and the literature is based mainly on two studies using two different contrast media to evaluate adrenal lesions. Indeed, Nagumo et al.<sup>2</sup> used Sonazoid as a contrast medium, while SonoVue was utilised both in Bargellini et al.<sup>15</sup> and in the present study. SonoVue and Sonazoid are the two most commonly used second-generation CEUS contrast media. The main difference between the two is that the former is entirely an intravascular agent whereas the latter is specifically phagocytosed by Kupffer cells in the liver. This particular characteristic of Sonazoid enables a longer (about 15 minutes) enhanced post-injection phase compared to SonoVue, the so-called Kupffer phase characterised by specific enhancement patterns.<sup>23</sup> To date, Sonazoid has been commercially available only in China, Japan, Korea and Norway. A few studies<sup>23,24</sup> have shown that the diagnostic performances of the two contrast media are comparable in terms of accuracy and safety. More specifically, Zhai et al.<sup>23</sup> reported sensitivity and specificity values of 84.6% and 95%, respectively, in detecting hepatocarcinoma when Sonazoid was used and 83.3% and 95%, respectively, when SonoVue was administered.

Another limitation of the present study is that a comparison between lesion and ultrasonographically normal adrenal tissue was not performed for the B-mode and CEUS evaluation. As a consequence, the enhancement degree was not classified in terms of hypo-, iso- or hyperenhancement because only the lesion was visible in almost all the B-mode images and CEUS examinations due to the relatively large dimensions of the lesions themselves compared to the remaining adrenal parenchyma.

Lastly, no histopathological examination of the tumours was performed in the present study, and the tumours were grouped according to cytology and diagnostic imaging. Furthermore, the patients were referred only for the CEUS and cytopathological examination and then returned to the referring veterinarian; therefore, we are not aware of the results of additional

procedures (such as biopsies or CTs) that were eventually performed on the patients. Cytology has been shown to be accurate in distinguishing PHEOs from cortical adrenal tumours.<sup>18</sup> However, the malignancy of cortical ATs cannot be assessed in the absence of cells with marked criteria of atypia, since adenocarcinomas may contain well-differentiated cells.<sup>25</sup> For this reason, CAC was diagnosed if the cells were atypical or, in the absence of criteria of atypia, if vascular invasion was identified. CA was diagnosed when the cells had no criteria of atypia and no vascular invasion was detected by US.

## CONCLUSIONS

The B-mode and CEUS features of different canine adrenal focal lesions have been described. In addition, an easy-to-use, machine-learning-based decision tree has been developed for classifying lesions based on their B-mode and CEUS features. CACs and PHEOs are characterised as non-homogeneous lesions with the presence of both hypoperfused areas and intralesional disordered microcirculation during CEUS examination. Furthermore, PHEOs are characterised by a faster transit of the contrast medium. CAs feature smaller dimensions and present as homogeneous lesions during CEUS examination. Nevertheless, histopathological examination is still necessary in order to obtain a certain diagnosis of adrenal lesions.

## AUTHOR CONTRIBUTIONS

Silvia Burti, Alessandro Zotti, Tommaso Banzato, Federico Bonsembiante and Margherita Bendazzoli conceived the project, and drafted and revised the manuscript. Giuseppe Rubini, Riccardo Orlandi and Paolo Bargellini performed the CEUS examinations, and drafted and revised the manuscript. Barbara Contiero conducted the data analysis and revised the manuscript.

## ACKNOWLEDGEMENTS

The present paper is part of a project funded by a research grant from the Department of Animal Medicine, Production and Health—MAPS, University of Padua, Italy: SID Banzato 2019 (€16,850; Application of deep-learning algorithms in pet animal diagnostic imaging) and DOR Banzato 2022.

## CONFLICT OF INTEREST STATEMENT

None of the authors has any conflicts of interest.

## DATA AVAILABILITY STATEMENT

The data that support the findings of this study are available on request from the corresponding author. The data are not publicly available due to privacy or ethical restrictions.

## ETHICS STATEMENT


As the data used in this study were collected during routine clinical activity, no ethical committee

approval was needed. Informed consent for personal data processing was obtained from the owners.

## ORCID

Riccardo Orlandi  <https://orcid.org/0000-0002-6544-0256>

Federico Bonsembiante  <https://orcid.org/0000-0002-2879-7117>

Tommaso Banzato  <https://orcid.org/0000-0002-1261-9033>

## REFERENCES

- Cook AK, Spaulding KA, Edwards JF. Clinical findings in dogs with incidental adrenal gland lesions determined by ultrasonography: 151 cases (2007–2010). *J Am Vet Med Assoc.* 2014;244(10):1181–5.
- Nagumo T, Ishigaki K, Yoshida O, Iizuka K, Tamura K, Sakurai N, et al. Utility of contrast-enhanced ultrasound in differential diagnosis of adrenal tumors in dogs. *J Vet Med Sci.* 2020;82(11):1594–601.
- Baum JJ, Boston SE, Case JB. Prevalence of adrenal gland masses as incidental findings during abdominal computed tomography in dogs: 270 cases (2013–2014). *J Am Vet Med Assoc.* 2016;249(10):1165–9.
- Grooters AM, Biller DS, Theisen SK, Miyabayashi T. Ultrasonographic characteristics of the adrenal glands in dogs with pituitary-dependent hyperadrenocorticism: comparison with normal dogs. *J Vet Intern Med.* 1996;10(3):110–5.
- Bertolini G, Furlanello T, De Lorenzi D, Caldin M. Computed tomographic quantification of canine adrenal gland volume and attenuation. *Vet Radiol Ultrasound.* 2006;47(5):444–8.
- Lee E, Choi BK, Lee SK, Choi J. 3.0-Tesla MRI of normal canine adrenal glands. *Vet Radiol Ultrasound.* 2022;63(2):206–15.
- Soulsby SN, Holland M, Hudson JA, Behrend EN. Ultrasonographic evaluation of adrenal gland size compared to body weight in normal dogs. *Vet Radiol Ultrasound.* 2015;56(3):317–26.
- Pagani E, Tursi M, Lorenzi C, Tarducci A, Bruno B, Mondino ECB, et al. Ultrasonographic features of adrenal gland lesions in dogs can aid in diagnosis. *BMC Vet Res.* 2016;12(1):1–9.
- Burti S, Zotti A, Rubini G, Orlandi R, Bargellini P, Bonsembiante F, et al. Contrast-enhanced ultrasound features of malignant focal liver masses in dogs. *Sci Rep.* 2020;10(1):1–12.
- Banzato T, Burti S, Rubini G, Orlandi R, Bargellini P, Bonsembiante F, et al. Contrast-enhanced ultrasonography features of hepatobiliary neoplasms in cats. *Vet Rec.* 2020;186(10):320.
- Nakamura K, Sasaki N, Murakami M, Bandula Kumara WR, Ohta H, Yamasaki M, et al. Contrast-enhanced ultrasonography for characterization of focal splenic lesions in dogs. *J Vet Intern Med.* 2010;24(6):1290–7.
- Burti S, Zotti A, Rubini G, Orlandi R, Bargellini P, Bonsembiante F, et al. Contrast-enhanced ultrasound features of focal pancreatic lesions in dogs. *Vet Rec.* 2022;191:1–12.
- Linta N, Pey P, Baron Toaldo M, Pietra M, Felici M, Bettini G, et al. Contrast-enhanced ultrasonography in dogs with inflammatory bowel disease. *J Vet Intern Med.* 2021;35(5):2167–76.
- Pey P, Vignoli M, Haers H, Duchateau L, Rossi F, Saunders JH. Contrast-enhanced ultrasonography of the normal canine adrenal gland. *Vet Radiol Ultrasound.* 2011;52(5):560–7.
- Bargellini P, Orlandi R, Dentini A, Paloni C, Rubini G, Fonti P, et al. Use of contrast-enhanced ultrasound in the differential diagnosis of adrenal tumors in dogs. *J Am Anim Hosp Assoc.* 2016;52(3):132–43.
- Pey P, Rossi F, Vignoli M, Duchateau L, Marescaux L, Saunders JH. Use of contrast-enhanced ultrasonography to characterize adrenal gland tumors in dogs. *Am J Vet Res.* 2014;75(10):886–92.
- Ferrandis I, Jakovljevic S, Aprea F, Corletto F. Effect of two sedative protocols and hepatosplenic disease on Doppler indices of splenic arteries in dogs: a preliminary study. *Vet J.* 2013;197(3):712–6.
- Bertazzolo W, Didier M, Gelain ME, Rossi S, Crippa L, Avallone G, et al. Accuracy of cytology in distinguishing adrenocortical tumors from pheochromocytoma in companion animals. *Vet Clin Pathol.* 2014;43(3):453–9.
- Choi US AT. Endocrine/neuroendocrine system. In: Raskin RE, Meyer DJ, editors. *Canine and feline cytology: a color atlas and interpretation guide.* 3rd ed. Elsevier; 2016. p. 430–52.
- Ohlerth S, O'Brien RT. Contrast ultrasound: general principles and veterinary clinical applications. *Vet J.* 2007;174(3):501–12.
- Yoshida O, Kutara K, Seki M, Ishigaki K, Teshima K, Ishikawa C, et al. Preoperative differential diagnosis of canine adrenal tumors using triple-phase helical computed tomography. *Vet Surg.* 2016;45(4):427–35.
- Gregori T, Mantis P, Benigni L, Priestnall SL, Lamb CR. Comparison of computed tomographic and pathologic findings in 17 dogs with primary adrenal neoplasia. *Vet Radiol Ultrasound.* 2015;56(2):153–9.
- Zhai HY, Liang P, Yu J, Cao F, Kuang M, Liu F-Y, et al. Comparison of SonoZoid and SonoVue in the diagnosis of focal liver lesions: a preliminary study. *J Ultrasound Med.* 2019;38(9):2417–25.
- He M, Zhu L, Huang M, Zhong L, Ye Z, Jiang T. Comparison Between SonoVue and SonoZoid contrast-enhanced ultrasound in characterization of focal nodular hyperplasia smaller than 3 cm. *J Ultrasound Med.* 2021;40(10):2095–104.
- Raskin RE, Meyer DJ. *Canine and feline cytology: a color atlas and interpretation guide.* 3rd ed. Elsevier; 2016.

**How to cite this article:** Burti S, Zotti A, Rubini G, Orlandi R, Bargellini P, Bonsembiante F, et al. Contrast-enhanced ultrasound features of adrenal lesions in dogs. *Vet Rec.* 2023;e2949. <https://doi.org/10.1002/vetr.2949>